Amperometric Detection of NH_3 by Aromatic SAM-Modified Graphene

Nesli Yagmurcukardes, Abdullah Bayram, Hasan Aydin, Mustafa Can, Serafettin Demic, Yaser Acikbas, and Cem Celebi

***Abstract*—Ammonia (NH_3) is a toxic substance resulting in various acute and chronic effects on individuals. NH_3 detection, monitoring methods, and detection tools are desperately needed. In this work, we improved the NH_3 sensing capabilities of grapheme (GP) films deposited by chemical vapor deposition (CVD) by modifying aromatic self-assembled monolayer (SAM) molecules such as 5-[(3-methylphenyl) (phenyl) amino] isophthalic acid (MeIPA) and 5-(diphenyl)amino] isophthalic acid (PhIPA) on amperometric detection method. Morphological investigations of the films were carried out by optical and scanning electron microscopy (SEM). Surface potential was characterized with Kelvin probe force microscopy (KPFM), and vibrational properties were characterized with Raman spectroscopy. MeIPA modification increased NH_3 uptake by two times compared to unmodified GP. The results indicated that the SAM modification enhanced NH_3 molecule adsorption and improved its periodic reversible and reproducible response using the amperometric detection system, indicating that SAM molecules might be a feasible probe for NH_3.**

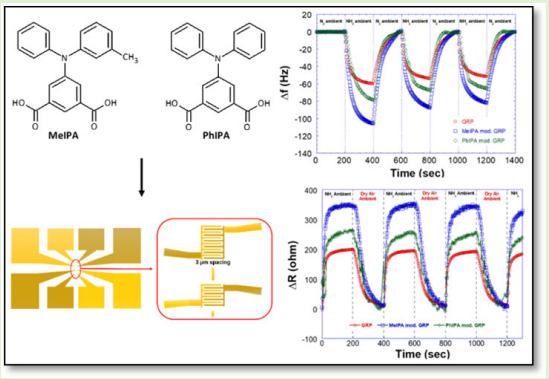

***Index Terms*— Ammonia (NH_3), amperometric detection, gas sensing, grapheme (GP), self-assembled monolayers (SAMs), self-assembly.**

Manuscript received 22 March 2023; accepted 29 March 2023. Date of publication 14 April 2023; date of current version 31 May 2023. This work was supported by the Scientific and Technological Research Council of Turkey (TUBITAK) under Project 112T946. The associate editor coordinating the review of this article and approving it for publication was Dr. Prasanta Guha. *(Corresponding author: Nesli Yagmurcukardes.)*

Nesli Yagmurcukardes is with the Department of Materials Science and Engineering, Izmir Institute of Technology, Izmir, TN 35430 USA, and also with the Department of Materials Science and Nanotechnology Engineering, Usak University, 64200 Usak, Turkey (e-mail: neslitekguzel@gmail.com).

Abdullah Bayram is with the Agricultural and Biological Engineering, Purdue University, West Lafayette, IN 47907 USA (e-mail: abdullahbayram7@gmail.com).

Hasan Aydin is with the Central Research Laboratories, Izmir Katip Celebi University, 35620 Izmir, Turkey (e-mail: aydinhasan1912@gmail.com).

Mustafa Can is with the Department of Engineering Sciences, Izmir Katip Celebi University, 35620 Izmir, Turkey (e-mail: mustafa.can@ikcu.edu.tr).

Serafettin Demic is with the Department of Metallurgical and Materials Engineering, Izmir Katip Celebi University, 35620 Izmir, Turkey (e-mail: serafettin.demic@ikcu.edu.tr).

Yaser Acikbas is with the Department of Materials Science and Nanotechnology Engineering, Faculty of Engineering, University of Usak, 64200 Usak, Turkey (e-mail: yaser.acikbas@usak.edu.tr).

Cem Celebi is with the Department of Physics, Quantum Device Laboratory, Izmir Institute of Technology, 35430 Izmir, Turkey (e-mail: cemcelebiphysics@gmail.com).

Digital Object Identifier 10.1109/JSEN.2023.3266167

I. Introduction

GRAPHENE (GP) has exhibited significant potential as a gas-sensing material due to its high specific surface area, unusual electrical properties, and reactivity to gas molecules in air conditions [1], [2], [3], [4]. GP's atomically small thickness makes carbon atoms linked firmly in a plane. Hence, each GP layer's atom is an activation site for gas interaction [2]. Because of its adjustable electrical conductivity and dipole coupling capacity, one electron in GP's orbital pz efficiently interacts with surrounding gas molecules. As a result, even a tiny variation in the GP surface state caused by sorption can modify its conductivity and generate response signals [5], [6]. Schedin et al. [2] published the first GP-based gas sensor, proving that absorbing a single gas molecule altered the number of charge carriers in the GP, which noticeably changed its electrical resistance in 2007. However, pristine GP has some significant limitations, including limited sensitivity, long response times, poor selectivity, and irreversible gas-sensing characteristic at ambient temperature. Numerous sensor operating methods of operating sensors have been investigated to improve gas-sensing properties, including external heaters, self-activation, metal oxides, polymer-based composites, and surface treatments employing functionalization or metal

decoration [7], [8], [9], [10], [11], [12], [13], [14], [15]. Among the techniques, functionalization has the benefit of acting as a receptor for specific activation while changing response behavior by altering the electronic structures. Nevertheless, GP (host) and adsorbing-molecule (guest) interactions rely on the chemical composition of interest. Among the variety of available gases such as O_2, NO_2, CO, CO_2, H_2, SO_2, H_2S, SO_2, and ammonia (NH_3), NH_3 has been extensively researched due to their industrial relevance and being one of the most toxic gases, capable of causing damage to the respiratory system, kidneys, eyes, skin, and liver when exposed to high quantities (>300 ppm) [16], [17]. While vital to our economy and supply of food, NH_3 is a dangerous gas to handle and store since it is very deadly and corrosive at all concentrations. Therefore, developing an NH_3 gas sensor is essential to prevent harm to living and environmental sustainability [18], [19], [20], [21], [22], [23], [24], [25], [26]. Notably, interest in GP-polyaniline (PANI) composites is gradually increasing since GP has exceptional electrical, thermal, and durable mechanical characteristics because of the distinct honeycomb structure of carbon atoms [27], [28], [29]. Tohidi et al. [30] developed a 3-D reduced graphene oxide (rGO)/PANI hybrid NH_3 sensor with a 50-ppm NH_3 response rate. A PANI hollow nanosphere composite on a polyethylene terephthalate (PET) substrate with a GO-rambutan-like structure was used by Li et al. [31] to build a room-temperature NH_3 sensor with a detection limit of 50 ppb.

Functionalization of GP via aromatic organic molecules, such as dye and self-assembled monolayers (SAMs), has advantages due to the nature of π–π stacking, which improves the GP's electronic properties. For instance, Midya et al. [32] and Kumar and Ghosh [33] described a novel method for detecting NH_3 selectively using rGO and rose bengal (an organic dye molecule), which probably had many functional groups for NH_3 binding. As a result, the rose bengal/rGO sensor responded to NH_3 more strongly than the rGO sensor individually. In addition, the Co-porphyrin/chemical vapor deposition (CVD)-G sensor demonstrated a sixfold higher sensitivity to NH_3 than unfunctionalized GP [34]. However, most dye molecules are toxic. At high concentrations, rose bengal has devastating effects on human corneal epithelium [35] and bromophenol blue on human pigmented epithelial cells [36]. SAMs can be a good choice for modifying GP surfaces in either covalent or noncovalent manners. For example, Wang et al. [37] developed an rGO-based NH_3 gas sensor using a self-assembly method to make conductive networks between Au electrodes. Wang et al. [37] also compared SAMs to pyrrole (Py) and hydrazine (Hy) molecules. The results showed that Py-rGO reacts to NH_3 much better than Hy-rGO, with a more than 2.7 times more robust response at 50 ppm. In another study, layer-by-layer self-assembly (LBL-SA) of graphene oxide (GO) on a single yarn was used to create a flexible textile-type NH_3 gas sensor. A poly (allylamine hydrochloride) (PAH) molecule was used as an SAM molecule. The single yarn-type NH_3 gas sensor made of the (GO/PAH)1 multilayer thin film improved sensing properties such as the high reaction (8.45 at 5 ppm NH_3), the excellent limit of detection (1.5 ppm), most extraordinary linearity ($R_2 = 0.9804$), a fast response time (68 s), and high selectivity [38]. However, there is still a lack of studies on GP functionalization via aromatic-based SAMs and the effects of aromatic SAMs on NH_3 gas-sensing properties.

This work investigates the effects of two different SAMs, 5-[(3-methylphenyl) (phenyl) amino] isophthalic acid (MeIPA) and 5-(diphenyl)amino] isophthalic acid (PhIPA), on GP's NH_3 gas-sensing capabilities. Optical microscopy and scanning electron microscopy (SEM) were used for structural characterization. The vibrational modes of GP films, their quality, and layer determinations were investigated by Raman spectroscopy. The contact potential differences and work function analysis were carried out by Kelvin probe force microscopy (KPFM). NH_3 sensing abilities were examined by quartz crystal microbalance (QCM) and amperometric measurements at both NH_3 and humid ambient.

II. Experimental Details

A. Materials

The 25-μm-thick Cu foils with 99.8% purity and S1318 photoresist (PR) were purchased from Alfa Easier Company and Microposit Company, respectively. AT-cut quartz crystals with 7.995-MHz oscillation frequency, 13.7 mm diameter, were used due to the temperature stability (Renlux Crystal Ltd.).

B. Synthesis of GP and Transfer Process

Initially, Cu foils, used as metal catalysts, were heated up to 1073 °C with a ramp rate of 32 °C/min under 20 standard cubic centimeters per minute (sccm) hydrogen (H_2) and 200 sccm argon (Ar) gas flow in the furnace tube. Then, Cu foils were annealed at 1073 °C for 1 h to eliminate the oxide layer from their top surfaces. GP growth was started by introducing 5 sccm of methane gas (CH_4) into the existing gas concentration for 3 min. The system was left cooling at an 18 °C/min rate using 20-sccm H_2 and 200-sccm Ar gas mixture to room temperature [39], [40], [41].

In the next step, GP layers on the Cu foils were transferred onto SiO_2/Si substrates and gold electrodes for characterization and amperometric investigations. During the transfer process, PR was used as a supporting layer to prevent the breaking or wrinkling of thin GP layers. PR was coated over GP/Cu substrate by drop-casting and annealed at 70 °C overnight. Iron(III) chloride ($FeCl_3$) is used as an etchant to get rid of the Cu substrate. After removing the entire Cu layer, the GP/PR structure was rinsed with deionized (DI) and dried with N_2. The GP/PR was conveyed to clean SiO_2/Si substrates and gold electrodes. To obtain better adhesion between GP and substrates, they were baked on a hot plate at 110 °C. Finally, GP/PR was immersed in hot acetone to remove the PR and create large area continuous GP films.

C. Preparation of MeIPA and PhIPA SAM Molecules

Aromatic small MeIPA and PhIPA SAM molecules with double-bond carboxylic acid (Fig. 1) were synthesized using a previously reported procedure [42]. SAM molecules solutions

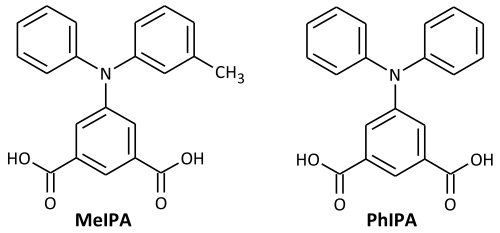

Fig. 1. Chemical structure of MeIPA and PhIPA SAM molecules.

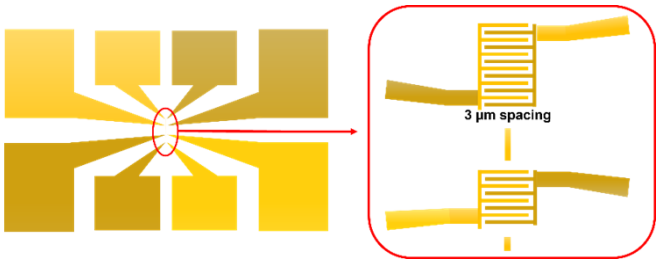

Fig. 2. Gold electrode pattern constructed by the photolithography process.

were prepared using methanol with a concentration of 1 mM at room temperature. The substrates with GP on top were stored in solution for a day to be fully coated by MeIPA and PhIPA molecules and then rinsed in methanol to remove residual molecules and dried with nitrogen.

D. Electrode Fabrication

Interconnected electrodes were fabricated by using photolithography. First, glass was used as a substrate and purified according to the standard cleaning procedure. They were rinsed in an ultrasonic bath with distilled water, acetone, ethanol, isopropanol, and distilled water for 15 min for each solvent. N_2 stream was applied to cleaned substrates to make them dry without leaving any stains. Oxygen plasma cleaning was utilized to eliminate other organic volatile residues. For metal film deposition, substrates were put into the thermal evaporation system. After the internal pressure of 10^{-1} torr was achieved initially to obtain good mechanical adhesion, thin chromium (Cr) layer and a 60-nm-thick gold layer were deposited. Photolithography was performed on these samples with thin metal films.

AZ1505 PR was used as a positive PR for microfabrication. PR was coated on the films at 4600 rpm for 50 s. Samples were cured with UV light for 3 s under the mask with a 3-μm width and 3-μm groves following 5-s soft baking at 90 °C on a hot plate. Then, the samples were processed with developer solution (AZ726 MIF) for 3 s to etch the PR layer. Samples were dipped into an Aqua Regia to etch the gold-deposited regions for 5 s and they were then rinsed with distilled water immediately to stop etching. The Cr etchant solvent also etched the excess amount of the Cr layer. The fabricated gold electrodes were rinsed by the same initial standard purification process (with DI water, ethanol, isopropanol, and DI water). The resulting pattern of the deposited gold electrodes is shown in Fig. 2.

Fig. 3. SEM images of GP layers on the interdigitated electrode with (a) 1-mm, (b) 100-μm, and (c) 10-μm scales.

E. Characterization of GP Films

SEM images of GP films on gold electrodes of quartz crystal were achieved by SEM [Field Electron and Ion Company (FEI) Quanta-250FEG environmental scanning electron microscopy (ESEM)] with an e-beam having a 5.00-kV accelerating voltage. Ar-ion type gas laser (purchased from Trivista and Princeton Instruments) was used to obtain the Raman spectrum of GP on gold electrodes. During the investigation, a laser with a 488-nm operating wavelength and a grating with 600 grooves per millimeter were used with a 100× microscope objective.

SAM modification of GP may be proven by measuring the surface potential difference. The potential surface investigations were carried out by atomic force microscope (AFM) and KPFM from NTMDT, using TiN as a cantilever with a 35-nm curvature radius. The conductive TiN AFM tip was used during the KPFM measurements. The relationship of the work function difference between the sample and the tip to the electric charge, e, is known as the surface potential difference [43]. Furthermore, the required minimum energy for discharging one e from the material's surface is expressed as the work function. The work function can be calculated with the following relation [44]:

$$W = 4.475 + \Delta W_{\text{sample}} - \Delta W_{\text{HOPG}} \tag{1}$$

where ΔW_{HOPG} is the work function variation of HOPG and AFM tip.

QCM measurement system setup was elaborated on in our previous study [41]. An electrochemical QCM system (CH Instruments, Austin, TX, USA) was used for the QCM test. Shortly, the system was settled by a two-channel gas flowmeter, a custom-made test cell, and a PC-controlled controller for the flow meters. Gas molecules' adsorption to the film surface leads to a frequency change that the Sauerbrey relation can analyze

$$\Delta f = \frac{-2f_0^2 \Delta m}{A\sqrt{\mu\rho}} \tag{2}$$

where QCM crystal's fundamental mode resonant frequency is expressed as f_0, A is the gold-coated area on the crystal, the crystal density is ρ, and μ is the shear modulus.

III. Results and Discussion

A. Morphological Analysis of GP Films

SEM images of transferred GP films onto the gold electrode part of the quartz crystal with three different magnifications are shown in Fig. 3. Successful and homogenous transfer of the GP layers is indicated by the contrast difference between the coated (dark) and uncoated (bright) regions.

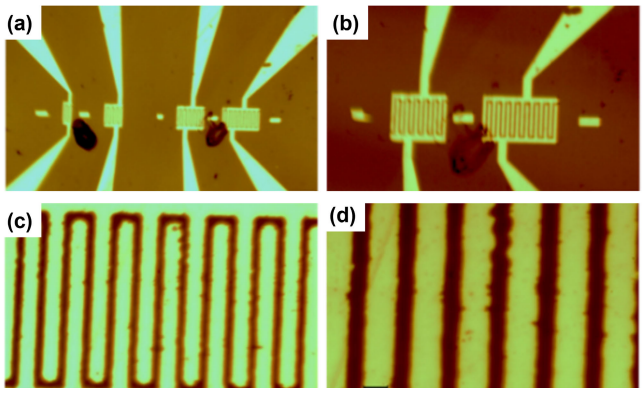

Fig. 4. Optical images of gold electrodes with (a) 5×, (b) 10×, (c) 50×, and (d) 100× magnifications.

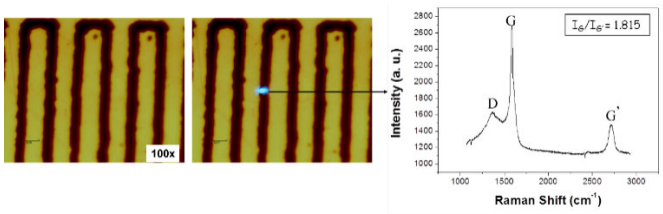

Fig. 5. GP layers microscope images with/without laser reflection. The laser was used for Raman analysis.

B. Optical Microscopy and Raman Spectra Analysis of GP

Optical images of the constructed gold electrodes are presented in Fig. 4 at 5×, 10×, 50×, and 100× magnifications. The scale bar in Fig. 4(d) corresponds to 3 μm in length, and the gold electrode's width and separation were measured as ∼3 μm.

The characterization of the vibrational properties of GP layers on gold electrodes was investigated by the Raman analysis. The spectrum obtained from the gap illuminated by a spot laser between two gold electrodes is presented in Fig. 5.

The ratio between G peak and G' peak intensity is used to extract layers' numbers of the GP film on the surface. The I_G ratio to $I_{G'}$ calculated from the spectra of the transferred GP layers was 1.815, indicating the presence of few-layered GP at the surface. In addition, the distinct D peak is evidence of some impurity effects that the organic solvent residuals may induce during the transfer process.

C. Kelvin Probe Force Microscopy Analysis of SAM-Modified GP

Bare graphene (GRP), MeIPA-modified GRP, and PhIPA-modified GRP's contact potential differences are given in Fig. 6. HOPG was used as the reference sample. The surface potentials measured from the curves as 0.130 V for unmodified GRP, 0.020 V for MeIPA-modified GRP, and 0.149 V for PhIPA-modified GRP.

As a result of the KPFM investigations, ΔW_{HOPG} was measured as 0.244 V. The work functions were measured as 4.13 eV for unmodified GRP, 4.25 eV for PhIPA-modified GRP, and 4.38 eV for MeIPA-modified GRP (see Table I).

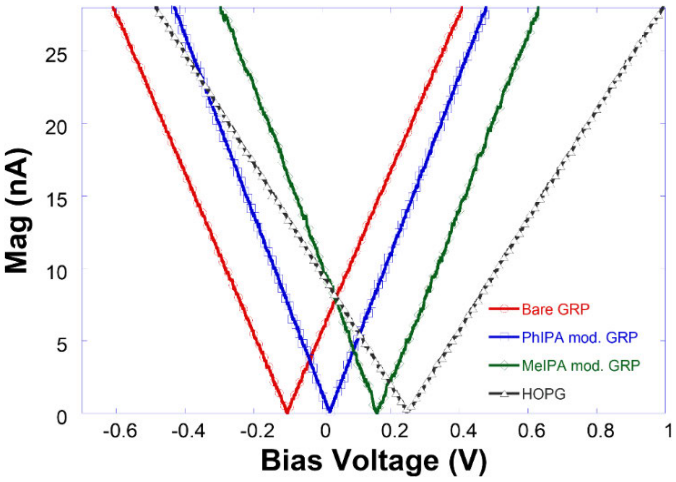

Fig. 6. Contact potential of GRP, modified GRPs, and reference.

TABLE I
CONTACT POTENTIAL DIFFERENCE AND WORK FUNCTIONS OF UNMODIFIED AND MODIFIED SAMPLES

Parameters	MeIPA mod. GRP	PhIPA mod. GRP	Bare GRP	HOPG
CPD (V)	0.149	0.020	0.103	0.244
Work function (eV)	4.25	4.38	4.13	4.47

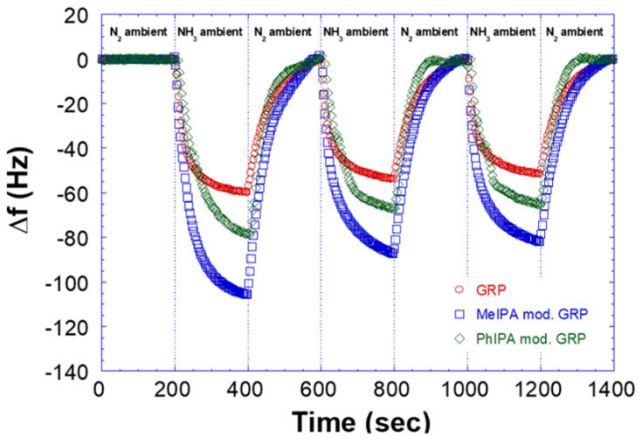

Fig. 7. NH_3 responses of bare GRP (red circles), MeIPA modified GRP (blue squares), and PhIPA modified GRP (green quadrangles) coated crystals under periodic N_2–NH_3 gas flows.

These results indicate that MeIPA-modified GRP had higher surface potential and work function values. Positive contact potential values of SAM-modified samples indicate that functionalization led to p-type doping. This type of doping makes surfaces more favorable for gas molecule adsorption.

D. Quartz Crystal Microbalance Analysis of Bare and SAM-Modified GP

The gas-sensing kinetics of bare GRP, MeIPA-modified, and PhIPA-modified GRPs subjected to NH_3 at room temperature were investigated and presented in Fig. 7. To analyze whether

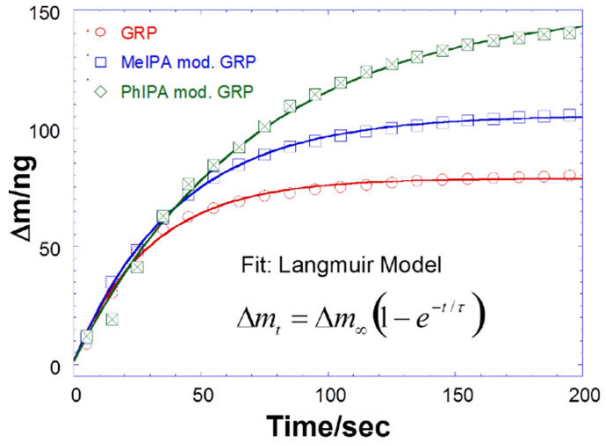

Fig. 8. Least squares fit (dashed lines) obtained by the Langmuir adsorption isotherm model for bare GRP-, MeIPA-, and PhIPA-modified GRP devices against NH_3.

TABLE II
LANGMUIR ADSORPTION ISOTHERM CONSTANTS HAVE BEEN DERIVED FOR NH_3

For N_2-NH_3	GRP	PhIPA mod. GRP	MeIPA mod. GRP
k_a	15.083	6.473	11.173
$\tau\ (s)$	331.495	772.418	447.5
k_d	$3.017e^{-03}$	$1.295e^{-03}$	$2.295e^{-03}$
$\Delta M_\infty\ (ng)$	86.541	166.881	115.951
R^2	0.9926	0.9904	0.9963
$R_{time}\ (s)90\%$	130	268	162

the films sustain reproducible and sensitive results, pure N_2 and NH_3 were purged repeatedly in 200-s periods through the testing cell. Initially, the QCM frequency counter was set to be stable around 0 Hz, and then, a 500-sccm flow of pure N_2 was supplied as a prior purification. The crystal's resonance frequency variation by desorption due to N_2 and adsorption due to NH_3 is correlated directly with the mass change on the QCM sensor.

The plots revealed that SAM-modified devices performed better sensitivity than the unmodified ones. The capability response was improved by nearly 60% in the MePIFA-modified sample. The PhIPA-modified sample also achieved almost 30% enhancement.

The absorption capability of NH_3 on GP surfaces was investigated by the Langmuir adsorption isotherm model, which explains gas molecules' interaction with a solid surface as forming a monolayer. The surface reaction rate is obtained from the following equations:

$$\frac{d\theta}{dt} = k_a\,(1-\theta)\,C - k_d\theta \tag{3}$$

where the surface covering percentage is represented by θ, the gas concentration in the air is represented by C, and the adsorption and desorption constants are shown by k_a and k_d, respectively. In addition, time-dependent fractional coverage of NH_3 molecules may be determined using the QCM approach. The following equation describes the relationship between the QCM frequency alteration (Δf) and the surface adsorption dynamics:

$$\Delta f(t) = \Delta f_{\max} K'(1 - e^{(k_a t)}). \tag{4}$$

The Sauerbrey equation can estimate the time-dependent alteration of adsorbed NH_3 molecules: $[\Delta m = -1.34(\text{ng/Hz})\cdot \Delta f]$ [45].

The Langmuir isotherm model's least squares fit (solid line) plot for NH_3 adsorption on both unmodified and modified GP surfaces is shown in Fig. 8. The parameters obtained from this fit plot are listed in Table II.

Δm_∞ corresponds to the maximum adsorbed gas molecules when the time approaches infinity. τ is the relation time required to release the molecule to 10% of its maximum gas uptake. It can be inferred from the table that adsorbed gas molecules and response time were increased with SAM modification. The SAM modification induced more available binding sites due to their molecular structures, and at room temperature, before any gas exposure started, the humidity molecules found in the experimental ambient bound to these sides. After NH_3 exposure was started, it took some time to recover and position the interchange of humid and NH_3 molecules. Consequently, increasing response time is expected. The sensitivity term is the rate of change in the detectable output based on the minimum physical parameter input. The response time is defined as the time to rise to 90% of the maximum value of the sensor signal, and the recovery time is defined as the time to fall to 10% of the maximum value of the sensor signal in that publication [46].

E. Amperometric Characterization of Bare and Modified GP

Within the scope of the amperometric characterization, the resistance response of devices was recorded during all ON/OFF cases of target gases. Resistivity variation of bare GRP sample during periodic N_2—NH_3 and dry air—NH_3 gas circulation with 200-s time periods is presented in Fig. 9. Adsorption causes gas molecules to shorten the electron flux, which enhances resistance. In an N_2 atmosphere and the presence of air molecules, bare GRP responded to NH_3 gas molecules quickly. The film's gas molecule adsorption capacities and repeatability are nearly equal after three cycles.

The resistivity response of bare GRP in a humid environment was investigated, as shown in Fig. 10. The humidity had little influence on the bare GRP device's electrical resistance. Thus, this may make it a suitable material for a gas detector.

In addition, in intermittent dry air and NH_3 ambient, the amperometric responses of unmodified and SAM-modified devices were tested. With the NH_3 flux, the resistivity responses of all the bare, MeIPA-modified, and PhIPA-modified GRP devices enhanced, indicating that the increased amount of target gas molecules adsorbed on the surfaces. The increased number of adsorbed gas molecules reduced the electrical conductivity. The recorded resistivity plots of GRP-, MEIPA-, and PhIPA-modified GRP samples with accumulated gas ambient are shown in Fig. 11. It is obvious that the highest

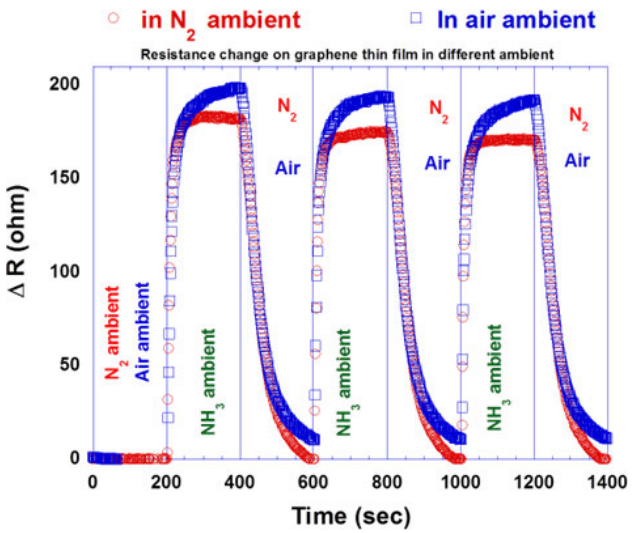

Fig. 9. Resistance alteration of bare GRP in periodic N_2–NH_3 (red circles) and periodic air–NH_3 (blue squares) flux.

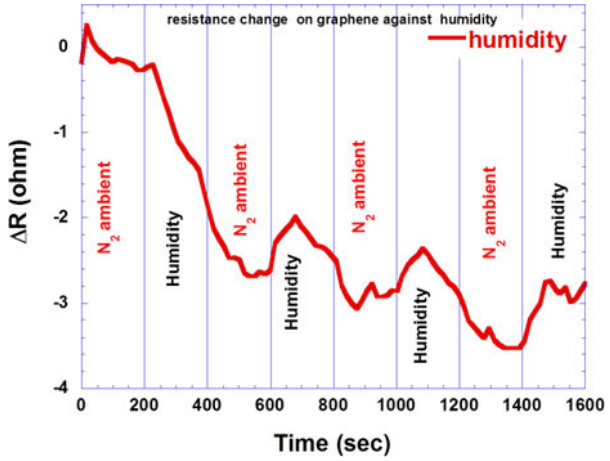

Fig. 10. Resistivity response of bare GRP in periodic N_2–humidity atmosphere.

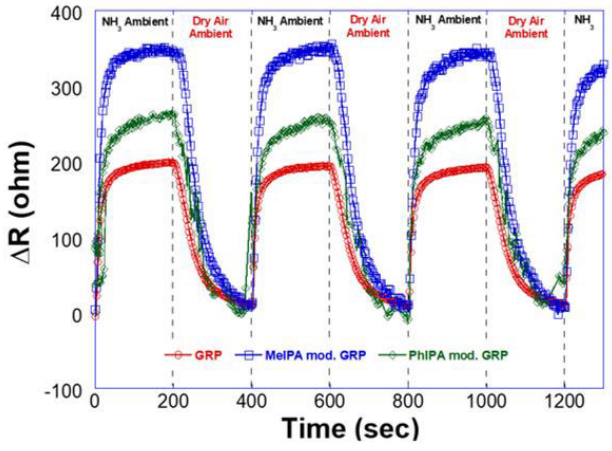

Fig. 11. Resistivity responses of bare GRP (red circles), MeIPA modified GRP (blue squares), and PhIPA modified GRP (green quadrangles) in periodic dry air–NH_3 atmosphere.

number of the adsorbed molecules is achieved with MeIPA-modified sample, which is also consistent with the QCM results.

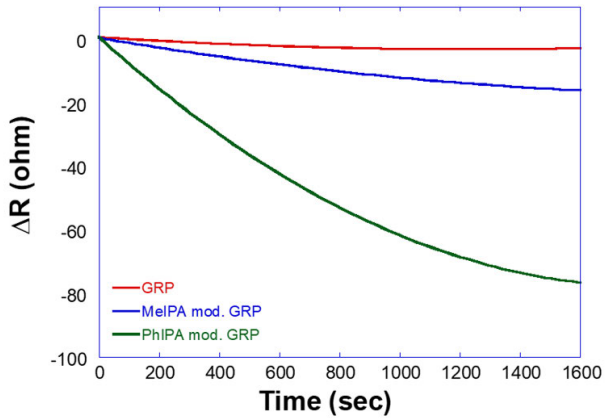

Fig. 12. Resistivity behavior of bare GRP, MeIPA modified, and PhIPA modified GRP in humid ambient.

The bare and modified samples' amperometric behavior was performed in a humid environment to exhibit the humidity sensitivity of the fabricated devices. The obtained plots are shown in Fig. 12.

According to the obtained plot, the PhIPA-modified GP device showed the highest sensitivity to humidity molecules. When NH_3 and humidity investigations are considered together, the MeIPA-modified GRP sample is the most appropriate for NH_3 sensing as it showed the highest NH_3 molecule adsorption and less humidity adsorption.

IV. Conclusion

Bare GRP-, MeIPA-, and PhIPA-modified GRP films with uniform morphology were successfully produced and transferred onto QCM crystals. Gold electrodes and their sensing abilities for toxic NH_3 gas were examined. In the kinetic studies, the reproducible behaviors of SAM-modified samples were demonstrated. Both QCM frequency and resistivity changes were used to capture device responses to explore the effects of humidity on device performances. An amperometric analysis was performed using constant I–V values and monitoring the resistance change brought on by the adsorption of the gas molecules. In QCM experiments, MEIPA-modified GRP devices with about 60% frequency augmentation in N_2–NH_3 environment and PhIPA-modified GP films with about 30% enhancement over bare GP showed the most significant improvement. SAM-modified samples once more outperformed unmodified GRP samples in the amperometric analysis. The MeIPA-modified device's resistivity was approximately 75% greater than the bare one, while the PhIPA-modified device improved by almost 25%. In conclusion, SAM-modified GRP sensors offer high sensitivity and good reproducibility for toxic NH_3 gas.

Acknowledgment

The authors would like to thank the Material Research Center, Izmir Institute of Technology, Izmir, Turkey, for their technical support in scanning electron microscopy (SEM) analysis.

References

[1] S. Basu and P. Bhattacharyya, "Recent developments on graphene and graphene oxide based solid state gas sensors," *Sens. Actuators B, Chem.*, vol. 173, pp. 1–21, Oct. 2012.

[2] F. Schedin et al., "Detection of individual gas molecules adsorbed on graphene," *Nature Mater.*, vol. 6, pp. 652–655, Jul. 2007.

[3] H. Song, X. Li, P. Cui, S. Guo, W. Liu, and X. Wang, "Sensitivity investigation for the dependence of monolayer and stacking graphene NH_3 gas sensor," *Diamond Rel. Mater.*, vol. 73, pp. 56–61, Mar. 2017.

[4] Y.-H. Zhang et al., "Improving gas sensing properties of graphene by introducing dopants and defects: A first-principles study," *Nanotechnology*, vol. 20, Apr. 2009, Art. no. 185504.

[5] O. Leenaerts, B. Partoens, and F. M. B. Peeters, "Adsorption of H_2O, NH_3, CO, NO_2, and NO on graphene: A first-principles study," *Phys. Rev. B, Condens. Matter*, vol. 77, no. 12, 2008, Art. no. 125416.

[6] O. Leenaerts, B. Partoens, and F. M. Peeters, "Adsorption of small molecules on graphene," *Microelectron. J.*, vol. 40, nos. 4–5, pp. 860–862, Apr. 2009.

[7] G. Lu et al., "Toward practical gas sensing with highly reduced graphene oxide: A new signal processing method to circumvent run-to-run and device-to-device variations," *ACS Nano*, vol. 5, no. 2, pp. 1154–1164, Jan. 2011.

[8] J. D. Fowler, M. J. Allen, V. C. Tung, Y. Yang, R. B. Kaner, and B. H. Weiller, "Practical chemical sensors from chemically derived graphene," *ACS Nano*, vol. 3, no. 2, no. 2, pp. 301–306, Jan. 2009.

[9] A. Lipatov, A. Varezhnikov, P. Wilson, V. Sysoev, A. Kolmakov, and A. Sinitskii, "Highly selective gas sensor arrays based on thermally reduced graphene oxide," *Nanoscale*, vol. 5, no. 12, pp. 5426–5434, Jun. 2013.

[10] M. W. K. Nomani et al., "Highly sensitive and selective detection of NO_2 using epitaxial graphene on 6H-SiC," *Sens. Actuators B, Chem.*, vol. 150, no. 1, pp. 301–307, Sep. 2010.

[11] K. Yu, P. Wang, G. Lu, K.-H. Chen, Z. Bo, and J. Chen, "Patterning vertically oriented graphene sheets for nanodevice applications," *J. Phys. Chem. Lett.*, vol. 2, no. 6, pp. 537–542, Mar. 2011.

[12] A. Kaniyoor, R. I. Jafri, T. Arockiadoss, and S. Ramaprabhu, "Nanostructured Pt decorated graphene and multi walled carbon nanotube based room temperature hydrogen gas sensor," *Nanoscale*, vol. 1, no. 3, pp. 382–386, 2009.

[13] H. Song, L. Zhang, C. He, Y. Qu, Y. Tian, and Y. Lv, "Graphene sheets decorated with SnO_2 nanoparticles: In situ synthesis and highly efficient materials for cataluminescence gas sensors," *J. Mater. Chem. A*, vol. 21, no. 16, pp. 5972–5977, 2011.

[14] J. Wang, S. Rathi, B. Singh, I. Lee, H.-I. Joh, and G.-H. Kim, "Alternating current dielectrophoresis optimization of Pt-decorated graphene oxide nanostructures for proficient hydrogen gas sensor," *ACS Appl. Mater. Interfaces*, vol. 7, no. 25, pp. 13768–13775, Jul. 2015.

[15] Y. H. Kim et al., "Chemically fluorinated graphene oxide for room temperature ammonia detection at ppb levels," *J. Mater. Chem. A*, vol. 5, no. 36, pp. 19116–19125, 2017.

[16] Z. Wu et al., "Enhanced sensitivity of ammonia sensor using graphene/polyaniline nanocomposite," *Sens. Actuators B, Chem.*, vol. 178, pp. 485–493, Mar. 2013.

[17] O. Braissant, "Ammonia toxicity to the brain: Effects on creatine metabolism and transport and protective roles of creatine," *Mol. Genet. Metabolism*, vol. 100, pp. S53–S58, Jan. 2010.

[18] M. Eising, C. E. Cava, R. V. Salvatierra, A. J. G. Zarbin, and L. S. Roman, "Doping effect on self-assembled films of polyaniline and carbon nanotube applied as ammonia gas sensor," *Sens. Actuators B, Chem.*, vol. 245, pp. 25–33, Jun. 2017.

[19] D. Lv, W. Shen, W. Chen, R. Tan, L. Xu, and W. Song, "PSS-PANI/PVDF composite based flexible NH_3 sensors with sub-ppm detection at room temperature," *Sens. Actuators B, Chem.*, vol. 328, Feb. 2021, Art. no. 129085.

[20] Q. Zhao et al., "Edge-enriched $Mo_2TiC_2T_x/MoS_2$ heterostructure with coupling interface for selective NO_2 monitoring," *Adv. Funct. Mater.*, vol. 32, no. 39, 2022, Art. no. 2203528.

[21] Y. Zhang et al., "Edge-enriched MoS_2 nanosheets modified porous nanosheet-assembled hierarchical In_2O_3 microflowers for room temperature detection of NO_2 with ultrahigh sensitivity and selectivity," *J. Hazardous Mater.*, vol. 434, Jul. 2022, Art. no. 128836.

[22] C. Liu et al., "Local Gaussian process regression with small sample data for temperature and humidity compensation of polyaniline-cerium dioxide NH_3 sensor," *Sens. Actuators B, Chem.*, vol. 378, Mar. 2023, Art. no. 133113.

[23] Q. Wu, W. Shen, D. Lv, W. Chen, W. Song, and R. Tan, "An enhanced flexible room temperature ammonia gas sensor based on GP-PANI/PVDF multi-hierarchical nanocomposite film," *Sens. Actuators B, Chem.*, vol. 334, May 2021, Art. no. 129630.

[24] J. Liu, N. Cui, Q. Xu, Z. Wang, L. Gu, and W. Dou, "High-performance PANI-based ammonia gas sensor promoted by surface nanostructuralization," *ECS J. Solid State Sci. Technol.*, vol. 10, no. 2, Feb. 2021, Art. no. 027007.

[25] X. Duan et al., "Enhanced NH_3 sensing performance of polyaniline via a facile morphology modification strategy," *Sens. Actuators B, Chem.*, vol. 369, Oct. 2022, Art. no. 132302.

[26] L. Kumar, I. Rawal, A. Kaur, and S. Annapoorni, "Flexible room temperature ammonia sensor based on polyaniline," *Sens. Actuators B, Chem.*, vol. 240, pp. 408–416, Mar. 2017.

[27] K. Vikrant, V. Kumar, and K.-H. Kim, "Graphene materials as a superior platform for advanced sensing strategies against gaseous ammonia," *J. Mater. Chem. A*, vol. 6, no. 45, pp. 22391–22410, 2018.

[28] N. Karim et al., "Scalable production of graphene-based wearable E-textiles," *ACS Nano*, vol. 11, no. 12, pp. 12266–12275, Dec. 2017.

[29] R. Alrammouz, J. Podlecki, P. Abboud, B. Sorli, and R. Habchi, "A review on flexible gas sensors: From materials to devices," *Sens. Actuators A, Phys.*, vol. 284, pp. 209–231, Dec. 2018.

[30] S. Tohidi, M. Parhizkar, H. Bidadi, and R. Mohamad-Rezaei, "High-performance chemiresistor-type NH_3 gas sensor based on three-dimensional reduced graphene oxide/polyaniline hybrid," *Nanotechnology*, vol. 31, no. 41, Oct. 2020, Art. no. 415501.

[31] S. Li et al., "Room temperature high performance NH_3 sensor based on GO-rambutan-like polyaniline hollow nanosphere hybrid assembled to flexible PET substrate," *Sens. Actuators B, Chem.*, vol. 273, pp. 726–734, Nov. 2018.

[32] A. Midya, R. Ghosh, S. Santra, S. K. Ray, and P. K. Guha, "Reduced graphene oxide–Rose Bengal hybrid film for improved ammonia detection with low humidity interference at room temperature," *Mater. Res. Exp.*, vol. 3, no. 2, Jan. 2016, Art. no. 025101.

[33] R. Kumar and R. Ghosh, "Selective determination of ammonia, ethanol and acetone by reduced graphene oxide based gas sensors at room temperature," *Sens. Bio-Sens. Res.*, vol. 28, Jun. 2020, Art. no. 100336.

[34] K. Sawada et al., "Co-porphyrin functionalized CVD graphene ammonia sensor with high selectivity to disturbing gases: Hydrogen and humidity," *Jpn. J. Appl. Phys.*, vol. 59, Apr. 2020, Art. no. SGGG09.

[35] H. M. Tabery, "Toxic effect of Rose Bengal dye on the living human corneal epithelium," *Acta Ophthalmol. Scand.*, vol. 76, no. 2, pp. 142–145, Apr. 1998.

[36] M.-C. Morales et al., "Comparative effects of six intraocular vital dyes on retinal pigment epithelial cells," *Investigative Ophthalmol. Vis. Sci.*, vol. 51, no. 11, pp. 6018–6029, 2010.

[37] Y. Wang et al., "Ammonia gas sensors based on chemically reduced graphene oxide sheets self-assembled on Au electrodes," *Nanosc. Res. Lett.*, vol. 9, no. 1, pp. 1–12, May 2014.

[38] P.-G. Su and Z.-H. Liao, "Fabrication of a flexible single-yarn NH_3 gas sensor by layer-by-layer self-assembly of graphene oxide," *Mater. Chem. Phys.*, vol. 224, pp. 349–356, Feb. 2019.

[39] H. Aydin et al., "Experimental and computational investigation of graphene/SAMs/n-Si Schottky diodes," *Appl. Surf. Sci.*, vol. 428, pp. 1010–1017, Jan. 2018.

[40] N. Yagmurcukardes et al., "Effect of aromatic SAMs molecules on graphene/silicon Schottky diode performance," *ECS J. Solid State Sci. Technol.*, vol. 5, no. 7, pp. M69–M73, 2016.

[41] N. Yagmurcukardes et al., "Anisotropic etching of CVD grown graphene for ammonia sensing," *IEEE Sensors J.*, vol. 22, no. 5, pp. 3888–3895, Mar. 2022.

[42] M. Can et al., "Electrical properties of SAM-modified ITO surface using aromatic small molecules with double bond carboxylic acid groups for OLED applications," *Appl. Surf. Sci.*, vol. 314, pp. 1082–1086, Sep. 2014.

[43] R. Kumar, D. Varandani, and B. R. Mehta, "Nanoscale interface formation and charge transfer in graphene/silicon Schottky junctions; KPFM and CAFM studies," *Carbon*, vol. 98, pp. 41–49, Mar. 2016.

[44] T. Yu, F. Wang, Y. Xu, L. Ma, X. Pi, and D. Yang, "Graphene coupled with silicon quantum dots for high-performance bulk-silicon-based Schottky-junction photodetectors," *Adv. Mater.*, vol. 28, no. 24, pp. 4912–4919, Jun. 2016.

[45] H. M. B. Darwish and S. Okur, "CO adsorption kinetics of ferrocene-conjugated polypyrrole using quartz microbalance technique," *Sens. Actuators B, Chem.*, vol. 200, pp. 325–331, Sep. 2014.

[46] A. Bayram, C. Özbek, M. Şenel, and S. Okur, "CO gas sorption properties of ferrocene branched chitosan derivatives," *Sens. Actuators B, Chem.*, vol. 241, pp. 308–313, Mar. 2017.

Nesli Yagmurcukardes received the B.Sc. and M.Sc. degrees from the Department of Physics and the Ph.D. degree in materials science and engineering from the Izmir Institute of Technology, Urla, Turkey, in 2008, 2011, and 2017, respectively.

Since 2021, she has been appointed as a Postdoctoral Researcher with Usak University, Uşak, Turkey. Her research interests include chemical gas sensors, biosensors, optoelectronic devices, scanning probe microscopy, and transmission electron microscopy analysis.

Abdullah Bayram received the B.Sc. degree in physics and the M.Sc. and Ph.D. degrees in materials science and engineering from the Izmir Institute of Technology, Urla, Turkey, in 2012, 2014, and 2018, respectively.

He is a Postdoctoral Researcher with Purdue University, West Lafayette, IN, USA. His research interests include chemical sensors, biosensors, and optofluidics.

Hasan Aydin received the Ph.D. degree in materials science and engineering from the Izmir Institute of Technology (IZTECH), Izmir, Turkey, in 2018.

His current research interests include 2-D materials and their optoelectronic and sensor applications, organic electronics, and scanning probe microscopy.

Mustafa Can received the B.S. degree from the Department of Chemistry and the Ph.D. degree from Ege University, Bornova, Turkey, in 2005 and 2012, respectively.

He is working under the supervision of Dr. Sıddık ICLI. As a Ph.D. Student, he worked in the area of organic chemistry, investigating new organic semiconductors for optoelectronic devices. His research interests include biosensors, optoelectronic devices, photoelectrochemical water splitting, and CO_2 reductions.

Serafettin Demic received the Ph.D. degree in organic chemistry from Ege University, Bornova, Turkey, in 2001.

After having different academic positions, he is currently with the Metallurgical and Materials Engineering Department, Izmir Katip Celebi University, Izmir, Turkey. He has expertise in organic syntheses, characterizations, and applications of organic-based materials used in optoelectronic technologies and water purification.

Yaser Acikbas was born in Turkey, in 1979. He received the B.Sc., M.Sc., and Ph.D. degrees in physics from the University of Balikesir, Balıkesir, Turkey, in 2003, 2006, and 2012, respectively.

He was appointed as an Assistant Professor and an Associate Professor with the Department of Materials Science and Nanotechnology Engineering, Usak University, Uşak, Turkey, in 2013 and 2017, respectively. His research interests include the fabrication of Langmuir–Blodgett (LB) thin films, chemical gas sensors based on organic nanomaterials, optical and swelling properties of nanothin films, and materials science applications.

Cem Celebi received the Ph.D. degree in applied physics from the Department of Eindhoven, University of Technology, Delft, The Netherlands, in 2009.

He is currently an Associate Professor with the Physics Department, IZTECH, Izmir, Turkey, where he is also the Principal Investigator and the Group Leader of the Quantum Device Laboratory.